Annu. Rev. Pharmacol. Toxicol. 2000. 40:431–58

NICOTINIC RECEPTORS AT THE AMINO ACID LEVEL

Pierre-Jean Corringer, Nicolas Le Novère, and Jean-Pierre Changeux

Neurobiologie Moléculaire, Unité de recherche associée au Centre National de la Recherche Scientifique D1284 Institut Pasteur, 75724 Paris Cedex 15, France; e-mail: changeux@pasteur.fr

Key Words nAChR, nicotinic, ion channel, allosteric proteins

■ **Abstract** nAChRs are pentameric transmembrane proteins into the superfamily of ligand-gated ion channels that includes the $5HT_3$, glycine, $GABA_A$, and $GABA_C$ receptors. Electron microscopy, affinity labeling, and mutagenesis experiments, together with secondary structure predictions and measurements, suggest an all-β folding of the N-terminal extracellular domain, with the connecting loops contributing to the ACh binding pocket and to the subunit interfaces that mediate the allosteric transitions between conformational states. The ion channel consists of two distinct elements symmetrically organized along the fivefold axis of the molecule: a barrel of five M2 helices, and on the cytoplasmic side five loops contributing to the selectivity filter. The allosteric transitions of the protein underlying the physiological ACh-evoked activation and desensitization possibly involve rigid body motion of the extracellular domain of each subunit, linked to a global reorganization of the transmembrane domain responsible for channel gating.

INTRODUCTION

Ligand-gated ion channels mediate intercellular communication by converting the neurotransmitter signal released from the nerve ending into a transmembrane ion flux in the postsynaptic neurone or muscle fiber. According to the classical scheme of fast ''wiring'' transmission, the neurotransmitter is released in the synaptic cleft at a high concentration (up to 0.3 mM) and brief pulse (approximately 1 ms) (1), whereas in the ''volume transmission'' or paracrine mode, lower concentrations of the neurotransmitter may more slowly reach a distant target through intercellular space (2). Nicotinic receptors for acetylcholine (nAChRs) may contribute, among the ligand-gated ion channels, to both types of chemical communication in relation to their topological distribution at the pre- and/or postsynaptic levels.

With the use of snake venom α-toxins (3), the identification and purification of the muscle-type electric fish nAChR (4–7) demonstrated that the isolated protein contains all of the structural elements required for chemo-electrical transduction. These physiological properties include the activation response to fast application of ACh in the millisecond timescale resulting in the opening of the ion channel, as well as the slow decrease or even full abolition of the electrical response referred to as desensitization, following a prolonged application of nicotinic agonists and antagonists. A substantial body of biochemical and electron microscopy data subsequently revealed that the nAChR is a heteropentamer, made up of four subunits α1, β1, γ, and δ, pseudosymmetrically arranged with a 2:1:1:1 stoichiometry (6).

The full amino acid sequence of the muscle type, and of several neuronal nAChR subunits have been available for nearly two decades, together with low-resolution three-dimensional (3D) electron microscopy data. Yet most of our knowledge on the functional organization of nAChR derives from affinity labeling and mutagenesis experiments. Crystallographic and nuclear magnetic resonance information of the nAChR molecule are still lacking. At this stage however, the body of available experimental and computational data appears sufficient to define an envelope of structural constraints that justifies the proposal of the general 3D organization of the ACh binding site and of the ion channel at the amino acid level, as plausible anticipations of the experimentally determined 3D structure.

THE nAChR OLIGOMER

The initial cloning (8–10) and sequencing (11–14) of *Torpedo* electric organ nAChR subunits paved the way for the identification of a family of homologous genes encoding nAChR subunits in muscle and brain that belongs to an even larger superfamily of ligand-gated ion channels (15), which includes the 5-HT_3 (16), $GABA_A$ (17), $GABA_C$ (18), and glycine receptors (19) in both vertebrate and invertebrate species [amino acid and nucleotide sequences of all the members of the superfamily can be found in Le Novère & Changeux (20)]. The complete sequence of the *Caenorhabditis elegans* genome revealed an unexpected wealth of genes (more than 40) coding for putative subunits in the nicotinic superfamily (21). Many of them are clearly orthologous to known vertebrate subunits. This is the case for ACR7,9,10,11,14,15,16 (Ce21) with α7,8 or ACR6,8,12,13 and UNC38 with α1–6, β1–4, γ, δ, ε. However, according to the sequence analysis, some of the newly discovered genes (for instance DEG3, ACR5, or F18G5.4) do not possess clear orthologs among the known vertebrate nAChR subunits. This would suggest that several new nAChR subunit genes might still be uncovered in the human genome.

The nAChR subunits genes fall into two main classes: The α subunits (α1–9) possess two adjacent cysteines essential for acetylcholine binding (22, 23), whereas the non-α referred to as β, γ, ε, or δ do not (24). Comparative analysis

of the available nAChR subunits gene sequences suggests that the first duplication between nAChR subunits is probably older than one and half billion years, whereas the last ones may have occurred around 400 million years ago (such as α7/α8 or β2/β4) (25, 26). The nAChR vertebrate subunits include the following subfamilies, defined on the basis of protein sequence and gene structure (position of the introns in the coding sequence): subfamily I, epithelial α9; subfamily II, neuronal α7,8; subfamily III, neuronal α2–6 and β2–4; and subfamily IV, muscle α1, β1, γ, δ, and ε. The subfamilies III and IV can be further subdivided, on the basis of sequence similarities, into three tribes: tribe III-1, α2,3,4,6; tribe III-2, β2,4; tribe III-3, α5, β3; tribe IV-1, α1; tribe IV-2, γ, δ, ε; and tribe IV-3, β1.

Reconstitution experiments in *Xenopus* oocytes and cultured mammalian cells have shown that for the subunits belonging to each subfamily, the assembly into functional oligomers follows well-defined rules. Members of subfamilies I and II, when expressed alone, are able to form functional homopentamers (27–30). These ancestral type receptors are presumably characterized by a perfect fivefold symmetry. In the case of the recently evolved subfamily III, the coexpression of one member of tribe III-1 and one member of tribe III-2 is required to form an ACh gated ion channel with a currently accepted stoichiometry of 2 α(s) for 3 β(s) (31, 32). Some of these receptors incorporate a third type of subunit from tribe III-3, either α5 (33, 34) or β3 (35). Finally, the assembly of the subunits from the highly evolved muscle subfamily IV appears tightly constrained with a fixed clockwise [α1-γ-α1-δ-β1] order of subunits (6, 36; but see 37).

The more promiscuous assembly of neuronal subunits generates a diversity of receptors, with 24 possible oligomer compositions theoretically generated on the basis of a contribution of one member of tribe III-1 and tribe III-2, plus zero or one member of tribe III-3, and with 14 oligomers actually observed in reconstituted systems. This results in a high diversity in pharmacological specificities, desensitization kinetics, and channel permeabilities, in particular to calcium ions (reviewed in 38), and in diverse cellular and subcellular distributions in the brain (39, 40). The spatiotemporal development of such rich patterns of nAChR gene expression requires complex transcriptional and posttranscriptional regulations, which can hardly be achieved with single promoter species (see 41). As suggested in the case of developmental genes (42, 43), the multiplication of promoters consecutive to gene duplication may allow a fine spatio-temporal control of transcription and thus tentatively explain such large diversity of subunit genes.

TRANSMEMBRANE ORGANIZATION AND SUBUNIT STRUCTURE

At low resolution by electron microscopy, the *Torpedo* receptor appears as an integral elongated transmembrane protein, that protrudes by ~60 and ~20 Å into the synaptic and intracellular compartments, respectively, with an apparent five-

fold axis of symmetry perpendicular to the membrane. It creates a central pore, with a diameter of ~25 Å at the synaptic entry, which becomes narrower at the transmembrane level (44) (Figure 1*B*).

Strong experimental evidence supports a commonly accepted transmembrane topology shared by all subunits (reviewed in 45) (Figure 1*A*): (*a*) an amino-terminal domain facing the extracellular environment, glycosylated, and carrying at least one highly conserved cysteine bridge (corresponding to α7 C128–C142); and (*b*) three transmembrane segments (20 amino acids)—M1, M2, and M3—separated by short loops, a large and variable intracellular domain and a fourth

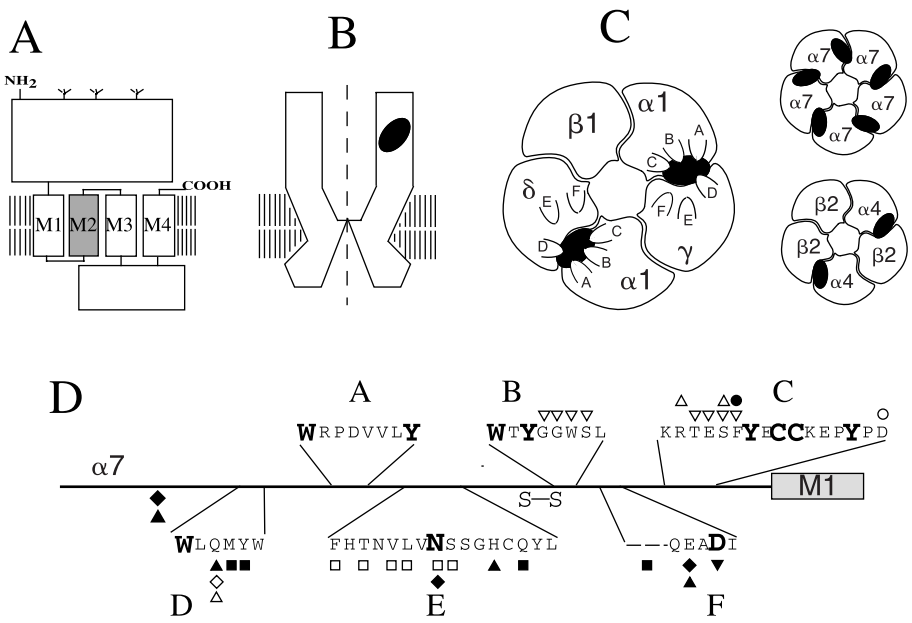

Figure 1 (*A*) The membrane topology of a typical nAChR subunit. (*B*) Schematic drawing of the nAChR in axial section. The ion channel is located along the axis of pseudo-symmetry of the molecule, and the binding site for ACh is shown (*shaded pocket*). (*C*) Schematic drawing of nAChRs in top view, illustrating the quaternary organization of the muscle-type receptor (*left panel*) and of the homooligomeric α7 and heterooligomeric α4β2 receptors (*right panel*). (*Shaded pockets*) The ACh binding sites at the subunit interfaces, contributed by loops A, B, and C of the ''principal component'' and loops D, E, and F of the ''complementary component.'' (*D*) Linear representation of the α7 N-terminal domain. (*Bold residues*) Correspond to those affinity labeled on the *Torpedo* receptor (see text). (*Symbols*) Labeled residues homologous to those contributing to the pharmacological diversity in the entire family of nAChR. (*Open symbols*) Neuronal receptors: *triangles* (86), *inverted triangles* (89), *squares* (96), *diamonds* (95), and *circles* (87); (*closed symbols*) muscle-type receptors: *triangles* (92), *inverted triangles* (91), *squares* (67, 93), *diamonds* (68), and *circles* (90).

transmembrane segment M4. The relatively short carboxy-terminal end is then extracellular. A refined prediction of the secondary structure of a typical nAChR subunit (46) has been computed using third-generation algorithms from an alignment of a representative set of 18 nAChR and $5HT_3$ subunit sequences. Incorporation of representative sequences of members of the superfamily carrying an anionic channel (glycine and $GABA_A$ receptors) yields similar predictions, indicating that all subunits from the family share almost identical secondary and tertiary structures. This was anticipated from their sequence similarities and from the observation that a chimera joining the N-terminal domain of the α7 nAChR to the transmembrane and cytoplasmic regions of the $5HT_3$ receptor mediates channel activation and desensitization by ACh (47).

Small-scale expression of peptide fragments corresponding to the entire N-terminal extracellular domain of the α1 or α7 subunits yields soluble proteins (48–51). Whereas the α1 fragment appeared to be in a monomeric state, the expression of the α7 fragments resulted in a soluble pentameric complex, which displays binding properties resembling those of the native receptor. Thus, the N-terminal domain may spontaneously fold and become stabilized into a native-like conformation, as long as the pentameric organization is preserved. Circular dichroism measurements on the soluble α1 extracellular portion reveals the abundance of β-strands (51% β-strand, 12% α-helix) (50). This reasonably agrees with the secondary structure predictions (31.7% β-strand, 13.7% α-helix), depicting two α-helices at the N terminus, followed by a large core of β-strands that extends to the transmembrane segment M1. An all-β portion was also identified by measuring the secondary structure of progressively deleted $GABA_A$ α1 subunits (52). Electron microscopy of *Torpedo* receptor at 7.5 Å resolution revealed two cavities located 30 Å above the bilayer surface, which were tentatively assigned to the ACh binding pocket (37), each surrounded by three rods, interpreted as α-helix. On the other hand, at higher resolution (4.6 Å), the pattern of density is more consistent with a seven-stranded β-sheet structure (53), in agreement with the suggested all-β portion.

The ~20–amino acid transmembrane segments M1, M2, M3, and M4 were initially thought to fold into an α-helical structure. Yet, circular dichroism measurements of the M1-M2-M3 portion of the receptor (54), infrared spectroscopy of the *Torpedo* receptor for which the extracellular portion was removed by enzymatic digestion (55), and secondary structure predictions (46) suggest a mixed α/β topology. Extensive mapping of the protein-lipid interfaces using the hydrophobic probes 3-trifluoromethyl-3-(m-iodophenyl) diazirin (TID) (56), 4'-(3-trifluoromethyl-3H-diazin-3-yl)-2'-tributyl stannyl benzyl benzoate (TID-BE) (57), diazofluorene (DAF) (58), cholesterol (59), and promegestone (60) demonstrated a labeling of the M4 as well as of the two third ''extracellular'' portion of M3, with a pattern of labeling consistent with an α-helix. The ''intracellular'' one third portion of M1 was also found labeled, but with a pattern inconsistent with either an α-helix or a β-strand. The only non–lipid-exposed segment is M2.

Strong evidence supports its folding in an α-helix and its contribution to the ion channel along the central axis of pseudosymetry of the molecule (see below).

The cytoplasmic domain is predicted to consist of two well-conserved amphipatic helices joined together by a stretch of variable length and sequence devoid of periodic structures (46). Recent electron microscopy images of the cytoplasmic domain reveal that one rod of density protrudes from each subunit, possibly corresponding to one of the predicted α-helices (53).

THE NICOTINIC BINDING SITES

The Nicotinic Binding Sites at Subunit Interface

Concerning both electric organ and muscle nAChR, the following evidence demonstrates the location of the binding site for nicotinic agonists and competitive antagonists at the α1/γ and α1/δ subunit interfaces (Figure 1*C*).

1. Affinity labeling experiments performed with a series of competitive antagonists of different chemical structures—such as the aryl-cation p-(dimethylamino) benzenediazonium fluoroborate (DDF) (61, 62), the alcaloid d-tubocurarine (dTC) (63), the polypeptide α-bungarotoxin (64) and with the agonist nicotine (65)—show that all probes label primarily the α1 subunits, and to a lesser extent the γ and δ subunits (10%–25% of the α1 subunit labeling).
2. Expression in cell lines of the α1 subunit with either the γ or δ subunits yields an ACh binding pocket with native pharmacology, whereas all other pairwise coexpressions or single expressions of subunit failed to give ACh binding sites (66).
3. The αγ and αδ dimers display marked pharmacological differences, particularly for α-conotoxin MI with a 10,000-fold higher affinity for the α1/δ compared with the α1/γ binding sites of mouse muscle-type receptor (whereas dTC displays a 100-fold preference for the α1/γ site) (67, 68).

The much stronger labeling of α1 compared with that of the γ and δ subunits supports an asymmetric location of the binding site with respect to the interface. We thus proposed to refer to the α1 subunits as carrying the ''principal component,'' and the δ or γ subunits as contributing to the ''complementary component'' of the nicotinic binding site (69).

The various residues that compose the principal component of the α1 subunit of the *Torpedo* receptor were identified by affinity labeling, proteolysis, and Edman degradation experiments. 4-(N-maleimido) benzyltrimethyl ammonium (22) labels C192 and C193, which form a rather unusual disulfide bridge within, or in close proximity to, the ACh binding site. DDF labels Y93 (loop A), W149 (loop B), and Y190, C192, and C193 (loop C), and in a weak but significant manner W86, Y151, and Y198 (62, 70). These amino acids are also the site of

incorporation of the other probes used to date: Y93 is labeled by ACh mustard (71); Y198, C192, and Y190 by nicotine (65); Y190, C192, and Y198 by dTC (63); and Y190 by lophotoxin (72). For the complementary component, the homologous γW55 and δW57 (loop D) were found labeled by nicotine and dTC, whereas the homologous γY111 and δR113 (loop E) were weakly but specifically labeled by dTC (73, 74). In order to identify negatively charged residues contributing to the stabilization of the cationic ligands, a probe 0.9 nm long, grafted onto the reduced C192–C193 disulphide bridge and reacting with aspartates and glutamates, was found to label δD165, δD180, and δE182 (75). Mutation of δD180 (loop F) to asparagine, and of the homologous γD174, but not of δD165 and δE182, was found to decrease the affinity for ACh (76).

Sequence comparison indicates a high conservation of the loop A, B, C, and D motifs in the binding site of neuronal nAChRs. The labeled residues from loops A, B, and C are indeed present in the α2,3,4,6 and α7,8 subunits, and the labeled residue from loop D in the β2,4 and α7,8 subunits. In the homooligomeric α7 receptor, as well as in the α7-V201–$5HT_3$ chimera, which carries the α7 binding site, mutation of the corresponding residues (W54, Y92, W149, and Y188) alters the apparent affinities of binding and activation of ACh, establishing their contribution to the ACh binding site (69, 77). Thus, in this case, the same subunit carries both the principal and the complementary components of binding (Figure 1*C*). In contrast to this conserved core of amino acids, the labeled residue from loop E appears highly variable, whereas the aspartate of loop F is conserved in all γ-, δ-, ε-, and α7 subunits [where it also contributes to ACh binding (78)], but not in β2,4.

Physical Chemistry of the ACh Binding

The binding site of ACh and nicotinic ligands thus includes a conserved core of aromatic residues, whose electron-rich side chains might provide stabilizing interactions with the cationic ligands. In agreement with this notion, mutations of α1Y93, α1Y190, and α1Y198 affect in the same way the apparent affinities of ACh and tetramethylammonium, which suggests that these tyrosine residues contribute to stabilization of the quaternary ammonium portion of ACh (79). Probing the contribution of these amino acids by incorporation of unnatural amino acids reveals a prominent role of the hydroxyl group and of the aromatic ring of α1Y93 and α1Y198, respectively, whereas the α1Y190 position is found to be too sensitive to structural modifications to be analyzed (80). At position α1W149, the 50% effective concentration (EC_{50}) for ACh correlates with the cation-π binding capability of a series of fluorinated tryptophan derivatives (81), which suggests that the indole side chain of W149 makes van der Waals contact (cation-π interactions) with the quaternary ammonium group of ACh. Three lines of evidence further support this notion: (*a*) incorporation of a tyrosine graft with a quaternary ammonium [Tyr-O-$(CH_2)_3$-$N(CH_3)_3{}^+$] group produces some constitutive activity, thus plausibly mimicking a bound agonist close to W149 (81); (*b*) for the α7

receptor, the ACh apparent affinity is particularly sensitive to mutation at this position, with a 100-fold increase in EC_{50} for W149F compared with a 10-fold increase for Y93F and Y190F (77); and (*c*) a survey of protein structures indicates that tryptophan presents the most potent cation-π binding site, especially in the case of acetylcholine esterase, within which the quaternary group of ACh makes van der Waals contact with W84 in the X-ray crystallographic structure (82).

Mutation of the homologous γD174 and δD180 to asparagine was also found to decrease the affinities for ACh and tetramethylammonium (76). It is noteworthy that two other aspartates from the principal binding component, α1D152 from loop B (83) and α1D200 from loop C (84), have been shown to decrease the ACh binding affinity when mutated to asparagine. This indicates that aspartates may provide an additional contribution to the stabilization of the ammonium ion, possibly through long-range electrostatic interactions. Finally, mutations such as γY111R and δR113Y, located within the highly variable loop E of the complementary binding component, alter primarily the apparent affinities for dTC and α-conotoxin M1, but not for ACh, indicating the specific contribution of this residue to the binding of these large antagonists (74).

Altogether, these data establish that ACh interacts with a cluster of electron-rich or charged aromatic and acidic amino acid side chains within the nicotinic site, which primarily stabilize the ammonium portion of the molecule.

Mapping the Pharmacological Diversity of nAChR Binding Sites

The pharmacological properties of nAChR vary markedly with subunit composition and species. For instance, the binding affinity of ACh for chick nAChR range from 5 nM (α4β2) to 1 μM (α7). Long- and short-chain α-toxins from snake venoms typically bind with subnanomolar affinities to the muscle-type receptor, whereas only long-chain toxins bind with high affinity to α7 receptor (85). The long-chain κ-bungarotoxin exclusively binds to the α2β2 receptor. α-Conotoxin MII binds specifically to the α3β2 receptor (86).

On the principal side of the site, the construction of α2,3, α7,8, and α4,7 chimeras showed that several segments from the N-terminal domain contribute to the different agonist pharmacologies of α2β2 and α3β2 (87), of α7,8 (88), and of α7 and α4β2 (89). A major role of the C-loop region was found with the 180–208 segment in α7,8 contributing to the relative ACh and DMPP (1,1-dimethyl-4-phenylpiperazinium) affinities, and the 195–215 in α2,3 or 183–191 in α7,4 contributing to the relative ACh and nicotine affinities. In contrast, the 152–155 segment (loop B) in α7,4 chimeras was shown to alter the pharmacology of all agonists, independent of their chemical structure (89). In parallel, some amino acids contributing to toxin binding were found near loop C. A glycosylation at this level was shown to interfere with α-bungarotoxin binding, thus rendering cobra and mongoose resistant to α-toxin (90). Furthermore, mutations at position V188, Y190, P197, and D200 were found to decrease the affinity of the short-

chain toxin from *Naja mossambica mossambica* (NmmI) affinity by 60- to 400-fold (91).

On the complementary side of the site, the amino acids involved in the pharmacological diversity were found in most cases located at the level of loops D, E, and F. Mapping the amino acids involved in the different affinities of dTC, α-conotoxin MI, NmmI, and carbamylcholine for the α1/γ, α1/δ, and α1/ε binding sites of the mouse muscle-type receptor underlined the contribution of variable residues at position $i + 2$, 3, or 4 from δW55, $i + 4$ or 6 from δY113, and $i - 2$ and $i + 1$ or 2 from δD180. However, two other amino acids outside these loops, δS36 and δK163, were shown to account for some of the differences (67, 68, 92–94). A residue from loop D and several residues from loop E determine, respectively, the different affinities of DHβE/α-conotoxin MII (86, 95) and the different sensitivities of cytisine for α3β2 and α3β4 (96).

Altogether, these studies support the notion that variable residues located in the vicinity of the affinity labeled amino acids are the major elements contributing to the pharmacological diversity of the nAChRs. The emerging picture is that the binding site consists of a conserved core of aromatic residues, and that variable amino acids neighboring these positions, as well as several amino acids from the nonconserved loop E and F, confer on each receptor subtype its individual pharmacological properties (Figure 1*D*).

Models of the Extracellular Domain and of the ACh Binding Pocket

In the past few years, two different models of the N-terminal domain appeared in the literature. With a hidden Markov model approach (sequence-sequence comparisons), Tsigelny et al (97) found local resemblance between the nAChR subunits and some members of the cupredoxin superfamily. They hypothesized a common fold and developed a 3D model on this basis. In parallel, Gready et al (98) used a threading approach (sequence-structure comparisons) to find possible templates for the glycine receptor α1 subunit. Although they did not find any significant match, they conducted a modeling work based on their highest hit, a SH2–SH3 domain.

Although a unique specific fold is not consistently found by fold recognition approaches, these methods are nevertheless informative. In the analysis we conducted with all the program available, most of the hits belonged to the all-β class of protein. The majority were β-sandwiches generally of the immunoglobulin type, which are consistently aligned with the predicted all-β part of the extracellular moiety of the nAChR subunit. Furthermore, the β-sandwiches of immunoglobulins are flanked at both ends by three loops, analogous to the three loops of the principal and complementary components of the nAChR binding site.

In Figure 2 (see color insert), we propose a plausible model of a typical nAChR N-terminal domain, based on the immunoglobulin structure. The topology cartoon (Figure 2*A*) depicts the arrangement of the predicted nAChR secondary structure

elements on the immunoglobulin fold. The A, B, and C components of the binding site would be located on the main β-sheet of the sandwich, whereas the components E and F would be on the side of the smallest sheet. The 60 first amino acids of the nAChR subunit being absent from the model, the D component is not mapped here. The artist's drawings (Figure 2*B*) tentatively assemble two subunits to account for the formation of the binding site at the interface. The main component of the binding site, on one subunit, would be distal to the lipidic membrane, whereas the complementary component, on the facing subunit, would be proximal to the membrane. Rather than being rod shaped, as often described, the extracellular part of a subunit would be flattened, the interfaces being tilted (in three dimensions) rather than strictly vertical and radial. An actual modeling study will be necessary to verify that the hypothesis described above can account for the large body of experimental data available.

THE ION CHANNEL

The Structural Organization of the Ion Channel

The ion channel was initially chemically identified by photoaffinity labeling with the channel blocker chlorpromazine. Chlorpromazine was found to label, in an agonist-dependent manner, a unique high-affinity site to which contribute all five the subunits of *Torpedo* receptor. The amino acids labeled within the M2 transmembrane segment by chlorpromazine (99–102) by triphenylmethyl phosphonium (103), Meproadifen mustard (104), TID (105), TID-BE (57), DAF (58), and Tetracain (106), as well as by the substituted cysteine accessibility method (SCAM) (23), are consistent with the notion that the ion channel is located along the axis of symmetry of the receptor oligomer, at the fivefold interface of the subunits, each subunit contributing by its M2 segment. The pattern of labeling, i.e. residues homologous to S240, I243/T244, L247/S348, T250/V251, L254, and E258/I259 of the α7 receptor, strongly supports the folding of M2 into an α-helix, in agreement with secondary structure predictions (46). Electron microscopy images of the open conformation of the channel identified five rods bordering the ion channel, attributed to the M2 segment (107). The axis of the rods are ~18 and ~11.5 Å from the axis of the pore, at the upper and lower faces, respectively, in agreement with a funnel-shaped pore with a minimal diameter of ~10 Å. SCAM experiments suggest in addition that the upper part of M1 contributes to the channel (108, 108a), possibly by intercalation between the M2 segment in the upper part.

The reactivity pattern of introduced cysteine side chains with the impermeant methane-thiosulfonate ethyltrimethyl ammonium applied either extra- or intracellularly supports the conclusion that the narrowest portion of the close and open channel is located at the cytoplasmic border of M2 (corresponding to α7K238 and α7I239) (109). The diameter of the narrowest portion of the channel in its

open conformation was formally estimated to fit a square 6.5 x 6.5 Å wide to accommodate the largest permeant ions (110). Furthermore, the accessibility pattern at this level no longer fits with an α-helix. Residues homologous to α7G236, α7E237, and α7K238 indeed react with the thiosulfonate reagents, a finding consistent with the secondary structure prediction, which proposes this region as an extended loop accessible to solvent.

The ion channel thus appears to be composed of two distinct structural domains: an upper ''α-helical component,'' which delimits both the wide portion of the pore and the pharmacological site for noncompetitive blockers; and a lower ''loop component,'' which contributes to the narrowest portion of the channel (Figure 3) (see also 113–115a).

The Functional Organization of the Ion Channel

The functional contribution of the identified labeled residues to channel block (by QX222) (111), as well as to the intrinsic conductance and ionic selectivity of the pore (112), was further specified by site-directed mutagenesis, pointing to the

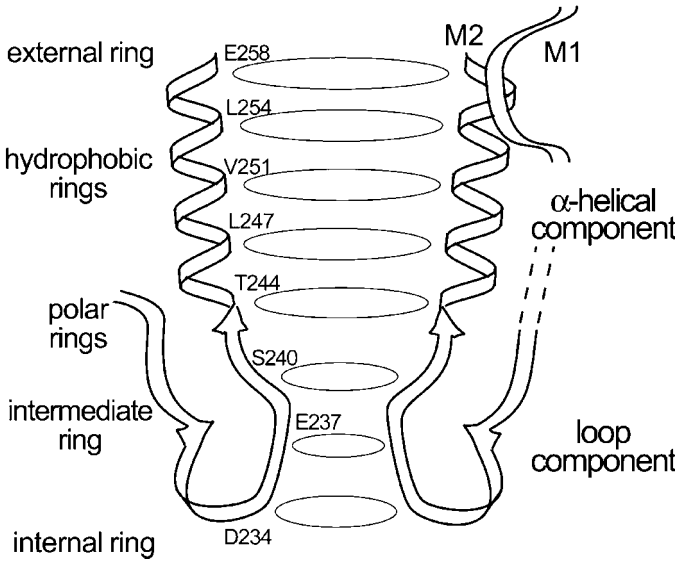

Figure 3 A model for the structural and functional organization of the ion channel. The contribution of two α7 subunits is shown to illustrate the ion channel, which is actually formed by homologous regions from the five subunits of the pentamer. The residues with numbers given are believed to face the lumen of the ion channel, thus forming rings of homologous residues (*circles*). The secondary structure of the M2 segment and M1–M2 loop is tentatively taken from Le Novère et al (46). The data accumulated to date suggest that the upper part of the channel, the α-helical component, acts as a water pore, whereas the lower loop component contributes to the selectivity filter of the ion channel.

contribution of two rings of polar Ser/Thr, three rings of hydrophobic Leu/Val, and three rings of charged Asp/Glu residues, which are highly conserved among the nAChR subunits sequenced to date.

So far, mutations within the loop component were found to alter all aspects of ionic selectivity of the channel:

1. Monovalent cation permeability and selectivity: In the muscle-type receptor, mutations in the rings corresponding to α7S240 and α7E237 progressively decrease the conductance of large cations when the volume of the side chain increases, which suggests that these residues are involved in cation selection according to their size (113–115); furthermore, in the muscle-type receptor, decreasing the net charge of the ring corresponding to α7E237 (and to a lesser extent to α7D234), results in a proportional decrease in potassium unitary conductance, in agreement with their direct or indirect (electrostatic) interaction with cations (116).
2. Divalent cation permeability: Mutation α7E237A abolishes the permeability of the α7 receptor to calcium but preserves that to monovalent cations (117).
3. Charge selectivity: The construction of chimeras between the cationic α7nAChR and the anionic α1GlyR shows that the insertion of a proline residue between positions 234 and 238 converts the selectivity of the E237A/V251T mutant of the α7 receptor from cationic to anionic (118, 119). Scanning mutagenesis indicates that no single residue within this loop is essential for anionic selectivity, stressing a major role of the loop conformation in the selectivity conversion. Yet the E237A mutation is required (but not sufficient) to yield an anionic channel, which suggests that this ring might constitute a negatively charged barrier to chloride ions.

At the level of the α-helical component, decreasing the net charge of the muscle-type ring corresponding to α7E258 results in a proportional decrease in potassium unitary conductance, yet to a lesser extent than in the case of α7E237 (116). At positions α7L247 and V251, introduction of polar or even charged residues is required, along with the proline insertion and the E237A mutation, to yield an anionic channel (118). However, in spite of anion-anion repulsion, mutation V251D also yields an anionic channel, indicating a mechanism not directly related to the nature of the side chain incorporated (119). A similar mechanism may occur in the case of the anionic $GABA_A$ homooligomeric receptor, for which introduction of a positively charged lysine at a position corresponding to α7A257 results in significant cationic permeability (120); also in the case of α7, mutations L254R or T and L255R, T, or G abolish the permeability to calcium (117).

The 10 Å diameter of the α-helical component is consistent with the notion that ions cross the membrane at this level in a fully hydrated state, whereas the narrower diameter of the loop component is expected to accommodate only partially dehydrated ions. The critical role of the loop component in cation discrimination as well as charge selectivity further supports its contribution to the selectivity filter of the channel by specific dehydration of ions. Accordingly, the

α-helical component would select on the basis of stabilization of hydrated ions within the membrane, and the several phenotypes observed at this level could be explained in a first attempt on the basis of a structural reorganization of this portion of the channel.

This conception of the nAChR ion channel is reminiscent of that of the tetrameric voltage-gated Na^+, Ca^{2+}, and K^+ channels, composed of similar components, but with an inverted disposition; the loop component (called P-loop) is located on the extracellular side (121), as established by X-ray crystallography in the case of a phylogenetically related bacterial potassium channel (122). Furthermore, the P-loop of the Na^+ and Ca^{2+} channels shows striking similarities with the loop component of nAChR: (*a*) It is made up of two rings of negatively charged residues separated by two amino acids analogous to α7D234/α7E237; and (*b*) mutation of the inner ring of Na^+ channel (DEKA) to the one of the Ca^{2+} channel (EEEE) confers Ca^{2+} permeability (123), which is reminiscent of α7E237A, which abolishes Ca^{2+} permeability (117). One may thus tentatively postulate that similar mechanisms of cation permeation operate in these rather structurally distant receptor channels.

Conjectures About the Three-Dimensional Organization of the Ion Channel

There exists very few resolved transmembrane structures of ionic channels, precluding the use of automated approaches to search possible templates for the nAChR transmembrane part. Synthetic peptides corresponding to the M2 segment of the α1 subunit form ionic pores within the membrane (124). These channels lack the loop component and thus are not likely to mediate ion permeation the same way the native receptor does. Nevertheless, structural model of the helical component was developed from the electron microscopy images (125), and from a minimization method of the channel blockers–M2 helices complexes (126). Also, on the basis of analogy arguments, Ortells et al (127) modeled the entire nAChR transmembrane portion based on the heat-labile enterotoxin B subunits.

Plausible templates are two recently resolved ion channels: the tetrameric potassium channel from *Streptomyces lividans* (1BL8) (122) and the pentameric mechanosensitive receptor from *Mycobacterium tuberculosis* (1MSL) (128) (Figure 2*C*). Both channels are formed by a bundle of inner α-helices arranged in a right-handed cone narrowing at its cytoplasmic side, which may resemble the α-helical component of nAChR formed by M2. However, a hypothetical model of nAChR based on the structure of 1BL8 would require its transformation into a pentamer. In contrast, the pentameric nature of the 1MSL channel fits the nAChR. Furthermore, the outer helices from this receptor contribute to the upper part of the pore, which suggests a possible analogy with the transmembrane segment M1 of nAChR. Using the inner/outer helices as a template for the M2/M1 segments requires a ''swap,'' where the connection between the helices is moved from the upper to the lower side of the channel (for examples of this type of circular

permutation, see 129). For the loop component, a plausible template could be generated by inverting the transmembrane organization of the potassium channel, thus locating its P-loop at the cytoplasmic border of the pore. The above proposed templates could guide the design of starting models, which would require further refinement by integrating the structural and functional data accumulated on the nAChR channel.

ALLOSTERIC TRANSITIONS OF THE nAChRS PROBED AT THE AMINO ACID LEVEL

The distance between the ACh binding sites and the ion channel, estimated to be 20–40 Å from fluorescence transfer measurements (130), is such that long-range ''allosteric'' interactions take place at the level of the nAChR oligomer in the course of the activation and desensitization processes. Agonists binding at topologically distant sites stabilize global conformations of the protein for which the channel is either open (activation) or closed (desensitization), depending on the concentration of the ligand and the kinetics of its application. With *Torpedo* nAChR-rich membranes, rapid mixing experiments following parallel fluorescent agonist binding and ion flux are consistent with a minimal four-state allosteric model, involving discrete B, A, I, and D states, where B is the low-affinity basal state that predominates in the absence of agonist, A is the active open-channel state, and I and D are desensitized states with, respectively, high (micromolar) and very high (nanomolar) dissociation constants (131, 132). Together with the in vivo results of patch clamp recordings (133), these in vitro data are adequately accounted for by an extended allosteric mechanism that involves a cascade of discrete two-state transitions (134–136).

In the case of hemoglobin, often referred to as the prototype of allosteric proteins (137, 138), X-ray structural data have demonstrated that the allosteric transitions that accompany oxygen binding are primarily associated with a reorganization of the quaternary structure with only minor changes in the tertiary structure of the subunits (see 137). In the case of nAChR, the physiologically important sites being located at the subunit interfaces, such global and rigid quaternary reorganizations, are expected to modify ''en bloc'' the binding site geometry and the state of opening of the ion channel. Consistent with these views, Unwin et al (44) have reported on the basis of the surface-on-views of *Torpedo* nAChR observed by cryoelectron microscopy that before and after equilibration with carbamylcholine, a desensitizing agonist, the whole δ subunit and to a large extent the γ subunit fall away from the pentagonal symmetry, as a consequence of a difference of inclination of 10° tangential to the receptor axis.

Structural Changes Within the N-Terminal Domain

The computed 2D representation of the N-terminal domain and the structural model suggest that this domain consists of a rigid core of β-strands with reduced structural flexibility. Furthermore, a large body of experimental data support the

notion that the allosteric transitions mediated by the nAChR molecule are associated with structural modifications of the subunit interfaces in the N-terminal domain: (*a*) Affinity labeling with DDF shows that, in the course of the B-to-D-state transition, the labeling of the loop A and B region increases, whereas that of the γ subunit increases and that of the δ subunit decreases (139). (*b*) Up to now, the mutations of the N-terminal domain that alter the allosteric transitions of the receptor were found at the level of the binding loops of the N-terminal domain that contribute to the subunit interface. For example, single-channel recordings of muscle-type nAChR mutants α1Y198F, εD175N, α1Y93F, and α1Y190F reveal alterations of the gating constants for ACh (140, 141), which may reflect changes of the isomerization constant of the protein between the B and A states. More striking, the mutation of residues 151–155 within loopB of α7, which causes an increase in binding affinity of agonists, alters primarily the isomerization constants leading to the desensitized states (89; see also 142). These mutations also alter the transition leading to the active state because their introduction of these mutations in the α7L247T mutant dramatically increases the fraction of receptor that spontaneously opens (PJ Corringer, JP Changeux & D Bertrand, unpublished observations). (*c*) The allosteric site for nAChR potentiation by Ca^{2+} was identified by scanning mutagenesis on the α7 receptor within the 161–172 segment, which carries loop F of the complementary component of the ACh binding site (78).

Thus, the currently available data are consistent with the view that the N-terminal domain of each subunit would undergo concerted rigid body motion during the allosteric transitions.

Structural Changes Within the Transmembrane Domain

The early observation that the channel blocker chlorpromazine photolabels its M2 site 1000 times faster when the channel is in its open configuration suggests that the α-helical component undergoes a structural reorganization during the activation process (99). Indeed, electron microscopy revealed that when nAChR rich membranes are rapidly mixed with very high concentrations (100 mM) of ACh, the five rods tentatively attributed to the M2 segments bend abruptly near the middle of the membrane and twist around the central axis in the lower part (107). However, SCAM experiments revealed that the residues that are exposed within this region of the pore do not significantly differ in the presence or absence of agonist (143). During desensitization, the labeling by channel blockers known to stabilize the B state [TID (105), TID-BE (57), tetracaine (106), and DAF (58)] shifts in the presence of a desensitizing agonist to a more expanded pattern that includes additional intracellular residues, a finding consistent with a widening of this region of the ionic pathway in the course of desensitization. Still, the same ''face'' of the helix is labeled both in the presence and in the absence of agonist.

Consistent with an important contribution of the α-helical component in the conformational transitions, mutations within α7 M2 profoundly alter the prop-

erties of both activation and desensitization (144). Increasing the polarity of the hydrophobic rings L247, V251, L254, and L255 results in pleiotropic phenotypes, which is well illustrated by the L247T mutation that results in (*a*) a shift of the ACh dose-response curve to lower concentrations, (*b*) a dramatic loss of desensitization, (*c*) the conversion of DHβE from an antagonist to a full agonist, and (*d*) the occurrence of spontaneous currents blocked by the competitive antagonist α-bungarotoxin (119, 144–147). In the case of the muscle-type nAChR, progressive replacement of homologous leucines leads to progressively larger shifts in the dose-response curves, with symmetrical effects on the α1, β, γ, and δ subunits (148). Congenital myasthenic syndromes were in many cases found to arise from single mutations within M2, generally characterized by prolonged ACh-evoked channel openings, and in some cases spontaneous openings or altered desensitization (149, 150). Autosomal dominant nocturnal frontal lobe epilepsy was also found to arise from mutations S247F and insertion of a leucine (776ins3) within M2 (151, 152) associated, in particular, with an altered agonist apparent affinity and desensitization (153, 154).

For the loop component of the ion channel, SCAM experiments on the α1 of the muscle nAChR indicate that residues corresponding to α7E237, K238, and I239 act as barriers to the permeant methanethiosulfonate ethylammonium when applied either extra- or intracellularly (109). Furthermore, the coapplication of methanethiosulfonate ethylammonium with ACh results in removal of this barrier, and within this region, the insertion of a proline between positions 233 and 238 in the α7 receptor, along with the E237A and V251T mutations, causes an increased ACh EC_{50} and high levels of spontaneous activity (119). These observations suggest that the loop component serves the double function of selectivity filter and physical gate of the channel in the B state. The above mentioned electron microscopy images, which suggest that the gate is located at the middle of the M2 α-helix (107), may thus have to be reinterpreted. Either the two segments making the ''kink'' do not belong to the same transmembrane segment or the kinked state corresponds to the desensitized rather than to the resting state.

The structural reorganization occurring along the entire length of the pore is, in addition, associated with a global rearrangement of the transmembrane domain.

First, in the M4 segment, mutations α1C418 and β1C447 (155) or γL440 and γM442 of the murine nAChR (156) alter the mean channel open time of ACh-evoked single-channel opening, without alteration of the unitary conductance. These residues belong to the lipid-exposed face of the M4 α-helix (56), supporting a strong link between channel gating and lipid-protein interaction. Along this line, several allosteric effectors of the *Torpedo* receptor were found to act at the lipid-receptor interface, as demonstrated directly by affinity labeling of lipid-exposed residues of M4 by the steroid noncompetitive antagonist promegestone (60). Mutation within M3 of V285I of the human α1 subunit causes a congenital myasthenic syndrome, characterized by single-channel slow opening and fast closing rates in the presence of ACh (157). Labeling experiments support the conclusion

that this residue faces the protein interior away from lipids (56). Internal protein motions thus also govern the gating mechanism.

Second, the transmembrane topology of the subunits supports the view that the upper part of M1, as well as the loop linking M2 and M3, may interact with the N-terminal domain, which suggests their possible contribution to the structural coupling between these two domains. In agreement with this idea, the highly conserved successive P and C residues at the middle of M1 were found to be involved in the gating mechanism, because mutation of the *Torpedo* γC230 alters the mean open time of ACh-evoked currents (158), and mutation of the murine receptor at α1P221 to L, A, or G, but not in β1, γ, or δ subunits, appeared nonfunctional electrophysiologically. Introducing at this position α-hydroxy acids corresponding to L, A, or G restores the receptor function, demonstrating that a backbone N-H group interferes with normal gating, probably through hydrogen bonding (159). At the middle of the M2–M3 loop, α7,3 chimeras revealed that mutation of α7D266 resulted in decreased agonist apparent affinities and maximally evoked currents (160). A mutation at this position (α1S269I) is also associated with a myasthenic syndrome, characterized by prolonged ACh-evoked channel openings (161).

In conclusion, many regions of the nAChR are involved in the allosteric transitions. The reorganization of the N-terminal domain is likely to be mainly associated with a change in quaternary structure. The transmembrane domain appear to undergo global conformational changes, associated with local changes at the level of both the α-helical and loop component of the pore, as well as at the lipid-protein interface. Both domains may be allosterically coupled by at least two segments located near the upper side of the membrane.

CONCLUSION

This overview of the nAChR illustrates the advances made in the understanding, at the amino acid level, of mechanisms underlying the chemico-electrical transduction mediated by the protein. In the absence of structural information at atomic resolution, the data presented lead to the proposal of plausible but still hypothetical structural models of the ACh binding sites and of the ion channel, ultimately accounting for their pharmacological and ionic selectivities, respectively. Furthermore, several aspects of the structural changes occurring during signal transduction have been presented involving mainly quaternary reorganizations.

Two mechanisms are currently used to fit nAChR data. On one hand, the Monod-Wyman-Changeux (MWC) theory (162, 163) postulates that the protein spontaneously isomerizes between discrete allosteric states characterized by ''all or none'' symmetrical changes. On the other hand, the sequential models (164, 165) postulate that the conformational transitions occur only after agonist binding, leading to agonist-induced multiple intermediate states. At this stage, it appears

difficult to discriminate unambiguously between these theories. Yet the following observations among others (see 135) support the MWC allosteric model.

1. Mutations altering receptor function and conformational transitions are found widely dispersed throughout the protein structure. In addition, mutations at discrete positions, such as α7L247T within the ion channel, modify the receptor properties in a pleiotropic manner, including the alteration of the apparent affinities of the far distant ACh binding sites. This indicates that global rather than local changes are associated with the transitions.
2. Mutations throughout the structure increase the frequency of spontaneously open states in the absence of ACh, unambiguously establishing that opening of the ion channel does not require, and thus is not induced by, ACh binding and supporting the occurrence of preexisting conformational equilibrium. The MWC theory, adapted to the nAChRs in an extended quantitative model (134), gives a general framework that directly accounts for such extremely pleiotropic phenotypes (166).

The subunit diversity of neuronal nAChRs is such that they may achieve a wide diversity of functions, such as fast wiring (phasic, α7 in CA1 interneurones of the hippocampus) and volume (tonic, α4β2 in CA1 interneurones of the hippocampus) transmission (167), according to both their intrinsic functional properties of activation and desensitization and their subcellular anatomical localization. Understanding these functions will require knowledge of the intimate biochemical and structural organization of these receptors, which has, and continues to, illuminate their physiology.

ACKNOWLEDGMENTS

We thank Stuart Edelstein for critical reading of the manuscript and valuable discussions, and Arthur Karlin and Denis Servent for useful suggestions. This work was supported by research grants from the Association Française contre les Myopathies, the Collège de France, the EEC Biotech and Biomed Programs, the Council for Tobacco Research, and the Reynolds Pharmaceuticals.

LITERATURE CITED

1. Katz B, Miledi R. 1977. Suppression of transmitter release at the neuromuscular junction. *Proc. R. Soc. London Ser. B* 196:465–69
2. Zoli M, Jansson A, Sykova E, Agnati LF, Fuxe K. 1999. Volume transmission in the CNS and its relevance for neuropsychopharmacology. *Trends Pharmacol. Sci.* 20:142–50
3. Lee CY, Chang CC. 1966. Modes of actions of purified toxins from elapid venoms on neuromuscular transmission. *Mem. Inst. Butantan Sao Paulo* 33:555–72

4. Changeux JP, Kasai M, Lee CY. 1970. The use of a snake venom toxin to characterize the cholinergic receptor protein. *Proc. Natl. Acad. Sci. USA* 67:1241–47
5. Changeux JP. 1991. Functional architecture and dynamics of the nicotinic acetylcholine receptor: an allosteric ligand-gated ion channel. *Fidia Res. Found. Neurosci. Award Lect.* 4:21–168
6. Karlin A. 1991. Explorations of the nicotinic acetylcholine receptor. *Harvey Lect. Ser.* 85:71–107
7. Lindstrom J. 1996. Neuronal nicotinic acetylcholine receptors. *Ion Channels* 4:377–450
8. Ballivet M, Patrick J, Lee J, Heinemann S. 1982. Molecular cloning of cDNA coding for the gamma subunit of *Torpedo* acetylcholine receptor. *Proc. Natl. Acad. Sci. USA* 79:4466–70
9. Giraudat J, Devillers-Thiery A, Auffray C, Rougeon F, Changeux JP. 1982. Identification of a cDNA clone coding for the acetylcholine binding subunit of *Torpedo marmorata* acetylcholine receptor. *EMBO J.* 1:713–17
10. Sumikawa K, Houghton M, Smith JC, Bell L, Richards BM, Barnard EA. 1982. The molecular cloning and characterisation of cDNA coding for the alpha subunit of the acetylcholine receptor. *Nucleic Acids Res.* 10:5809–22
11. Noda M, Takahashi H, Tanabe T, Toyosato M, Furutani Y, et al. 1982. Primary structure of alpha-subunit precursor of *Torpedo californica* acetylcholine receptor deduced from cDNA sequence. *Nature* 299:793–97
12. Noda M, Takahashi H, Tanabe T, Toyosato M, Kikyotani S, et al. 1983. Primary structures of beta- and delta-subunit precursors of *Torpedo californica* acetylcholine receptor deduced from cDNA sequences. *Nature* 301:251–55
13. Claudio T, Ballivet M, Patrick J, Heinemann S. 1983. Nucleotide and deduced amino acid sequences of *Torpedo Californica* acetylcholine receptor gamma-subunit. *Proc. Natl. Acad. Sci. USA* 80:1111–15
14. Devillers-Thiery A, Giraudat J, Bentaboulet M, Changeux JP. 1983. Complete mRNA coding sequence of the acetylcholine binding alpha-subunit of *Torpedo marmorata* acetylcholine receptor: a model for the transmembrane organization of the polypeptide chain. *Proc. Natl. Acad. Sci. USA* 80:2067–71
15. Cockcroft VB, Osguthorpe DJ, Barnard EA, Friday AE, Lunt GG. 1992. Ligand-gated ion channels: homology and diversity. *Mol. Neurobiol.* 4:129–69
16. Fletcher S, Barnes NM. 1998. Desperately seeking subunits: Are native 5-HT_3 receptors really homomeric complexes? *Trends Pharmacol. Sci.* 19:212–15
17. Macdonald RL, Olsen RW. 1994. $GABA_A$ receptor channels. *Annu. Rev. Neurosci.* 17:569–602
18. Bormann J, Feigenspan A. 1995. $GABA_C$ receptors. *Trends Neurosci.* 18:515–19
19. Bechade C, Sur C, Triller A. 1994. The inhibitory neuronal glycine receptor. *BioEssays* 16:735–44
20. Le Novère N, Changeux JP. 1999. The ligand gated ion channel database. *Nucleic Acids Res.* 27:340–42
21. Mongan NP, Baylis HA, Adcock C, Smith GR, Sansom MS, Sattelle DB. 1998. An extensive and diverse gene family of nicotinic acetylcholine receptor alpha subunits in *Caenorhabditis elegans. Recept. Channels* 6:213–28
22. Kao PN, Dwork AJ, Kaldany RRJ, Silver ML, Widemann J, et al. 1984. Identification of the alpha-subunit half-cystine specifically labeled by an affinity reagent for acetylcholine receptor binding site. *J. Biol. Chem.* 259:11662–65
23. Karlin A, Akabas MH. 1995. Toward a structural basis for the function of nicotinic acetylcholine receptors and their cousins. *Neuron* 15:1231–44
24. Sargent PB. 1993. The diversity of neu-

ronal nicotinic acetylcholine receptors. *Annu. Rev. Neurosci.* 16:403–43
25. Le Novère N, Changeux JP. 1995. Molecular evolution of the nicotinic acetylcholine receptor: an example of multigene family in excitable cells. *J. Mol. Evol.* 40:155–72
26. Ortells MO, Lunt GG. 1995. Evolutionary history of the ligand-gated ion-channel superfamily of receptors. *Trends Neurosci.* 18:121–27
27. Couturier S, Bertrand D, Matter JM, Hernandez MC, Bertrand S, et al. 1990. A neuronal nicotinic acetylcholine receptor subunit (alpha 7) is developmentally regulated and forms a homo-oligomeric channel blocked by alpha-BTX. *Neuron* 5:845–56
28. Schoepfer R, Conroy WG, Whiting P, Gore M, Lindstom J. 1990. Brain alpha-bungarotoxin binding protein cDNAs and MAbs reveal subtypes of this branch of the ligand-gated ion channel gene superfamily. *Neuron* 5:35–48
29. Gerzanich V, Anand R, Lindstrom J. 1994. Homomers of alpha 8 and alpha 7 subunits of nicotinic receptors exhibit similar channel but contrasting binding site properties. *Mol. Pharmacol.* 45:212–20
30. Elgoyhen AB, Johnson DS, Boulter J, Vetter DE, Heinemann S. 1994. Alpha 9: an acetylcholine receptor with novel pharmacological properties expressed in rat cochlear hair cells. *Cell* 79:705–15
31. Cooper E, Couturier S, Ballivet M. 1991. Pentameric structure and subunit stoichiometry of a neuronal nicotinic acetylcholine receptor. *Nature* 350:235–38
32. Anand R, Conroy WG, Schoepfer R, Whiting P, Lindstrom J. 1991. Neuronal nicotinic acetylcholine receptors expressed in Xenopus oocytes have a pentameric quaternary structure. *J. Biol. Chem.* 266:11192–98
33. Ramirez-Latorre J, Yu CR, Qu X, Perin F, Karlin A, Role L. 1996. Functional contribution of alpha5 subunit to neuronal acetylcholine receptor channels. *Nature* 380:347–51
34. Wang F, Gerzanich V, Wells G, Anand R, Peng X, et al. 1996. Assembly of human neuronal nicotinic receptor alpha5 subunits with alpha3, beta2, and beta4 subunits. *J. Biol. Chem.* 271:17656–65
35. Groot-Kormelink PJ, Luyten WH, Colquhoun D, Sivilotti LG. 1998. A reporter mutation approach shows incorporation of the ''orphan'' subunit beta 3 into a functional nicotinic receptor. *J. Biol. Chem.* 273:15317–20
36. Machold J, Weise C, Utkin Y, Tsetlin V, Hucho F. 1995. The handedness of the subunit arrangement of the nicotinic acetylcholine receptor from *Torpedo californica. Eur. J. Biochem.* 234:427–30
37. Unwin N. 1996. Projection structure of the nicotinic acetylcholine receptor: distinct conformations of the alpha subunits. *J. Mol. Biol.* 257:586–96
38. Role LW, Berg DK. 1996. Nicotinic receptors in the development and modulation of CNS synapses. *Neuron* 16:1077–85
39. Wada E, Wada K, Boulter J, Deneris E, Heinemann S, et al. 1989. Distribution of alpha2, alpha3, alpha4, and beta2 neuronal nicotinic receptor subunit mRNAs in the central nervous system: a hybridization histochemical study in the rat. *J. Comp. Neurol.* 284:314–35
40. Le Novère N, Zoli M, Changeux JP. 1996. Neuronal nicotinic receptor alpha6 subunit mRNA is selectively concentrated in catecholaminergic nuclei of the rat brain. *Eur. J. Neurosci.* 8:2428–39
41. Kerszberg M, Changeux JP. 1994. A model for reading morphogenetic gradients: autocatalysis and competition at the gene level. *Proc. Natl. Acad. Sci. USA* 91:5823–27
42. Li X, Noll M. 1994. Evolution of distinct developmental functions of three *Drosophila* genes by acquisition of different cis-regulatory regions. *Nature* 367:83–87
43. Xue L, Noll M. 1996. The functional

conservation of proteins in evolutionary alleles and the dominant role of enhancers in evolution. *EMBO J.* 15:3722–31
44. Unwin N, Toyoshima C, Kubalek E. 1988. Arrangement of the acetylcholine receptor subunits in the resting and desensitized states, determined by cryoelectron microscopy of crystallized *Torpedo* postsynaptic membranes. *J. Cell Biol.* 107:1123–38
45. Hucho F, Tsetlin VI, Machold J. 1996. The emerging three-dimensional structure of a receptor. The nicotinic acetylcholine receptor. *Eur. J. Biochem.* 239:539–57
46. Le Novère N, Corringer PJ, Changeux JP. 1999. Improved secondary structure predictions for a nicotinic receptor subunit. Incorporation of solvant accessibility and experimental data into a 2D representation. *Biophys. J.* 76:2329–45
47. Eiselé JL, Bertrand S, Galzi JL, Devillers-Thiéry A, Changeux JP, Bertrand D. 1993. Chimeric nicotinic-serotoninergic receptor combines distinct ligand binding and channel specificities. *Nature* 366:479–83
48. Schrattenholz A, Pfeiffer S, Pejovic V, Rudolph R, Godovac-Zimmermann J, Maelicke A. 1998. Expression and renaturation of the N-terminal extracellular domain of *Torpedo* nicotinic acetylcholine receptor alpha-subunit. *J. Biol. Chem.* 273:23393–99
49. Wells GB, Anand R, Wang F, Lindstrom J. 1998. Water-soluble nicotinic acetylcholine receptor formed by alpha7 subunit extracellular domains. *J. Biol. Chem.* 273:964–73
50. West AP, Bjorkman PJ, Dougherty DA, Lester HA. 1997. Expression and circular dichroism studies of the extracellular domain of the alpha subunit of the nicotinic acetylcholine receptor. *J. Biol. Chem.* 272:25468–73
51. Alexeev T, Krivoshein A, Shevalier A, Kudelina I, Telyakova O, et al. 1999. Physicochemical and immunological studies of the N-terminal domain of the *Torpedo* acetylcholine receptor alpha-subunit expressed in *Escherichia coli. Eur. J. Biochem.* 259:310–19
52. Xue H, Hang J, Chu R, Xiao Y, Li H, et al. 1999. Delineation of a membrane-proximal beta-rich domain in the $GABA_A$ receptor by progressive deletions. *J. Mol. Biol.* 285:55–61
53. Miyazawa A, Fujiyoshi Y, Stowell M, Unwin N. 1999. Nicotinic acetylcholine receptor at 4.6 Å resolution: transverse tunnels in the channel wall. *J. Mol. Biol.* 288:765–86
54. Corbin J, Methot N, Wang HH, Baenziger JE, Blanton MP. 1998. Secondary structure analysis of individual transmembrane segments of the nicotinic acetylcholine receptor by circular dichroism and Fourier transform infrared spectroscopy. *J. Biol. Chem.* 273:771–77
55. Gorne-Tschelnokow U, Strecker A, Kaduk C, Naumann D, Hucho F. 1994. The transmembrane domains of the nicotinic acetylcholine receptor contain alpha-helical and beta structures. *EMBO J.* 13:338–41
56. Blanton MP, Cohen JB. 1994. Identifying the lipid-protein interface of the *Torpedo* nicotinic acetylcholine receptor: secondary structure implications. *Biochemistry* 33:2859–72
57. Blanton MP, McCardy EA, Huggins A, Parikh D. 1998. Probing the structure of the nicotinic acetylcholine receptor with the hydrophobic photoreactive probes [^{125}I]TID-BE and [^{125}I]TIDPC/16. *Biochemistry* 37:14545–55
58. Blanton MP, Dangott LJ, Raja SK, Lala AK, Cohen JB. 1998. Probing the structure of the nicotinic acetylcholine receptor ion channel with the uncharged photoactivable compound [^{3}H]diazofluorene. *J. Biol. Chem.* 273:8659–68
59. Corbin J, Wang HH, Blanton MP. 1998. Identifying the cholesterol binding domain in the nicotinic acetylcholine

receptor with [^{125}I]azido-cholesterol. *Biochim. Biophys. Acta* 1414:65–74
60. Blanton MP, Xie Y, Dangott LJ, Cohen JB. 1999. The steroid promegestone is a noncompetitive antagonist of the *Torpedo* nicotinic acetylcholine receptor that interacts with the lipid-protein interface. *Mol. Pharmacol.* 55:269–78
61. Langenbuch-Cachat J, Bon C, Goeldner M, Hirth C, Changeux JP. 1988. Photoaffinity labeling by aryldiazonium derivatives of *Torpedo marmorata* acetylcholine receptor. *Biochemistry* 27: 2337–45
62. Dennis M, Giraudat J, Kotzyba-Hibert F, Goeldner M, Hirth C, et al. 1988. Amino acids of the *Torpedo marmorata* acetylcholine receptor subunit labeled by a photoaffinity ligand for the acetylcholine binding site. *Biochemistry* 27:2346–57
63. Pedersen SE, Cohen JB. 1990. d-Tubocurarine binding sites are located at the alpha-gamma and alpha-delta subunit interfaces of the nicotinic acetylcholine receptor. *Proc. Natl. Acad. Sci. USA* 87:2785–89
64. Oswald RE, Changeux JP. 1982. Crosslinking of alpha-bungarotoxin to the acetylcholine receptor from *Torpedo marmorata* by ultraviolet light irradiation. *FEBS Lett.* 139:225–29
65. Middleton RE, Cohen JB. 1991. Mapping of the acetylcholine binding site of the nicotinic acetylcholine receptor: [^{3}H]nicotine as an agonist photoaffinity label. *Biochemistry* 30:6987–97
66. Blount P, Merlie JP. 1989. Molecular basis of the two nonequivalent ligand binding sites of the muscle nicotinic receptor. *Neuron* 3:349–57
67. Sine SM. 1993. Molecular dissection of subunit interfaces in the acetylcholine receptor: identification of residues that determine curare selectivity. *Proc. Natl. Acad. Sci. USA* 90:9436–40
68. Sine SM, Kreienkamp HJ, Bren N, Maeda R, Taylor P. 1995. Molecular dissection of subunit interfaces in the acetylcholine receptor: identification of determinants of alpha-conotoxin M1 selectivity. *Neuron* 15:205–11
69. Corringer PJ, Galzi JL, Eiselé JL, Bertrand S, Changeux JP, Bertrand D. 1995. Identification of a new component of the agonist binding site of the nicotinic alpha 7 homooligomeric receptor. *J. Biol. Chem.* 270:11749–52
70. Galzi JL, Revah F, Black D, Goeldner M, Hirth C, Changeux JP. 1990. Identification of a novel amino acid alpha-Tyr 93 within the active site of the acetylcholine receptor by photoaffinity labeling: additional evidence for a three-loop model of the acetylcholine binding site. *J. Biol. Chem.* 265:10430–37
71. Cohen JB, Sharp SD, Liu WS. 1991. Structure of the agonist-binding site of the nicotinic acetylcholine receptor. *J. Biol. Chem.* 266:23354–64
72. Abramson SN, Li Y, Culver P, Taylor P. 1989. An analog of lophotoxin reacts covalently with Tyr 190 in the alpha-subunit of the nicotinic acetylcholine receptor. *J. Biol. Chem.* 264:12666–72
73. Chiara DC, Middleton RE, Cohen JB. 1998. Identification of tryptophan 55 as the primary site of [^{3}H]nicotine photoincorporation in the gamma-subunit of the *Torpedo* nicotinic acetylcholine receptor. *FEBS Lett.* 423:223–26
74. Chiara DC, Xie Y, Cohen JB. 1999. Structure of the agonist-binding sites of the *Torpedo* nicotinic acetylcholine receptor: affinity-labeling and mutational analyses identify gamma Tyr-111/delta Arg-113 as antagonist affinity determinants. *Biochemistry* 38:6689–98
75. Czajkowski C, Karlin A. 1995. Structure of the nicotinic receptor acetylcholine-binding site. Identification of acidic residues in the delta subunit within 0.9 nm of the 5 alpha subunit-binding. *J. Biol. Chem.* 270:3160–64
76. Martin M, Czajkowski C, Karlin A. 1996. The contributions of aspartyl residues in the acetylcholine receptor gamma

and delta subunits to the binding of agonists and competitive antagonists. *J. Biol. Chem.* 271:13497–503
77. Galzi JL, Bertrand D, Devillers-Thiéry A, Revah F, Bertrand S, Changeux JP. 1991. Functional significance of aromatic amino acids from three peptide loops of the alpha 7 neuronal nicotinic receptor site investigated by site-directed mutagenesis. *FEBS Lett.* 294:198–202
78. Galzi JL, Bertrand S, Corringer PJ, Changeux JP, Bertrand D. 1996. Identification of calcium binding sites that regulate potentiation of a neuronal nicotinic acetylcholine receptor. *EMBO J.* 15: 5824–32
79. Sine SM, Quiram P, Papanikolaou F, Kreienkamp HJ, Taylor P. 1994. Conserved tyrosines in the alpha subunit of the nicotinic acetylcholine receptor stabilize quaternary ammonium groups of agonists and curariform antagonists. *J. Biol. Chem.* 269:8808–16
80. Nowak MW, Kearney PC, Sampson JR, Saks ME, Labarca CG, et al. 1995. Nicotinic receptor binding site probed with unnatural amino acid incorporation in intact cells. *Science* 268:439–42
81. Zhong W, Gallivan JP, Zhang Y, Li L, Lester HA, Dougherty DA. 1998. From ab initio quantum mechanics to molecular neurobiology: a cation-π binding site in the nicotinic receptor. *Proc. Natl. Acad. Sci. USA* 95:12088–93
82. Sussman J, Harel M, Frolow F, Oefner C, Goldman A, et al. 1991. Atomic structure of acetylcholinesterase from *Torpedo californica:* a prototypic acetylcholine-binding protein. *Science* 253: 872–79
83. Sugiyama N, Boyd AE, Taylor P. 1996. Anionic residue in the alpha-subunit of the nicotinic acetylcholine receptor contributing to subunit assembly and ligand binding. *J. Biol. Chem.* 271:26575–81
84. O'Leary ME, White MM. 1992. Mutational analysis of ligand-induced activation of the *Torpedo* acetylcholine receptor. *J. Biol. Chem.* 267:8360–65
85. Servent D, Winckler-Dietrich V, Hu HY, Kessler P, Drevet P, et al. 1997. Only snake curaremimetic toxins with a fifth disulfide bond have high affinity for the neuronal alpha7 nicotinic receptor. *J. Biol. Chem.* 272:24279–86
86. Harvey SC, McIntosh JM, Cartier GE, Maddox FN, Luetje CW. 1997. Determinants of specificity for alpha-conotoxin MII on alpha3beta2 neuronal nicotinic receptors. *Mol. Pharmacol.* 51:336–42
87. Luetje CW, Piattoni M, Patrick J. 1993. Mapping of ligand binding sites of neuronal nicotinic acetylcholine receptors using chimeric alpha subunits. *Mol. Pharmacol.* 44:657–66
88. Anand R, Nelson ME, Gerzanich V, Wells GB, Lindstrom J. 1998. Determinants of channel gating located in the N-terminal extracellular domain of nicotinic alpha7 receptor. *J. Pharmacol. Exp. Ther.* 287:469–79
89. Corringer PJ, Bertrand S, Bohler S, Edelstein SJ, Changeux JP, Bertrand D. 1998. Critical elements determining diversity in agonist binding and desensitization of neuronal nicotinic acetylcholine receptors. *J. Neurosci.* 18:648–57
90. Kreienkamp HJ, Sine SM, Maeda RK, Taylor P. 1994. Glycosylation sites selectively interfere with alpha-toxin binding to the nicotinic acetylcholine receptor. *J. Biol. Chem.* 269:8108–14
91. Ackermann EJ, Taylor P. 1997. Nonidentity of the alpha-neurotoxin binding sites on the nicotinic acetylcholine receptor revealed by modification in alpha-neurotoxin and receptor structures. *Biochemistry* 36:12836–44
92. Prince RJ, Sine SM. 1996. Molecular dissection of subunit interfaces in the acetylcholine receptor. Identification of residues that determine agonist selectivity. *J. Biol. Chem.* 271:25770–77
93. Bren N, Sine SM. 1997. Identification of

residues in the adult nicotinic acetylcholine receptor that confer selectivity for curariform antagonists. *J. Biol. Chem.* 272:30793–98
94. Osaka H, Malany S, Kanter JR, Sine SM, Taylor P. 1999. Subunit interface selectivity of the alpha-neurotoxins for the nicotinic acetylcholine receptor. *J. Biol. Chem.* 274:9581–86
95. Harvey SC, Luetje CW. 1996. Determinants of competitive antagonist sensitivity on neuronal nicotinic receptor beta subunits. *J. Neurosci.* 16:3798–806
96. Figl A, Cohen BN, Quick MW, Davidson N, Lester HA. 1992. Regions of beta 4.beta 2 subunit chimeras that contribute to the agonist selectivity of neuronal nicotinic receptors. *FEBS Lett.* 308:245–48
97. Tsigelny I, Sugiyama N, Sine SM, Taylor P. 1997. A model of the nicotinic receptor extracellular domain based on sequence identity and residue location. *Biophys. J.* 73:52–66
98. Gready JE, Ranganathan S, Schofield PR, Matsuo Y, Nishikawa K. 1997. Predicted structure of the extracellular region of ligand-gated ion-channel receptors shows SH2-like and SH3-like domains forming the ligand-binding site. *Protein Sci.* 6:983–98
99. Heidmann T, Changeux JP. 1984. Time-resolved photolabeling by the noncompetitive blocker chlorpromazine of the acetylcholine receptor in its transiently open and closed ion channel conformations. *Proc. Natl. Acad. Sci. USA* 81:1897–901
100. Giraudat J, Dennis M, Heidmann T, Chang JY, Changeux JP. 1986. Structure of the high-affinity site for noncompetitive blockers of the acetylcholine receptor: serine-262 of the delta subunit is labeled by [^{3}H]chlorpromazine. *Proc. Natl. Acad. Sci. USA* 83:2719–23
101. Giraudat J, Galzi JL, Revah F, Changeux JP, Haumont PY, Lederer F. 1989. The noncompetitive blocker chlorpromazine labels segment MII but not segment MI on the nicotinic acetylcholine receptor alpha-subunit. *FEBS Lett.* 253:190–198
102. Revah F, Galzi JL, Giraudat J, Haumont PY, Lederer F, Changeux JP. 1990. The noncompetitive blocker [^{3}H]chlorpromazine labels three amino acids of the acetylcholine receptor gamma subunit: implications for the alpha-helical organization of the M2 segments and the structure of the ion channel. *Proc. Natl. Acad. Sci. USA* 87:4675–79
103. Hucho F, Oberthür W, Lottspeich F. 1986. The ion channel of the nicotinic acetylcholine receptor is formed by the homologous helices MII of the receptor subunits. *FEBS Lett.* 205:137–42
104. Pedersen SE, Sharp SD, Liu WS, Cohen JB. 1992. Structure of the noncompetitive antagonist-binding site of the *Torpedo* nicotinic acetylcholine receptor. [^{3}H]meproadifen mustard reacts selectively with alpha-subunit Glu-262. *J. Biol. Chem.* 267:10489–99
105. White BH, Cohen JB. 1992. Agonist-induced changes in the structure of the acetylcholine receptor M2 regions revealed by photoincorporation of an uncharged nicotinic noncompetitive antagonist. *J. Biol. Chem.* 267:15770–83
106. Middleton RE, Strand NP, Cohen JB. 1999. Photoaffinity labeling the *Torpedo* nicotinic acetylcholine receptor with [^{3}H]tetracaine, a nondesensitizing noncompetitive antagonist. *Mol. Pharmacol.* 56:290–99
107. Unwin N. 1995. Acetylcholine receptor channel imaged in the open state. *Nature* 373:37–43
108. Akabas MH, Karlin A. 1995. Identification of acetylcholine receptor channel-lining residues in the M1 segment of the alpha-subunit. *Biochemistry* 34:12496–500
108. (a) Zhang H, Karlin A. 1997. Identification of acetylcholine receptor channel-lining residues in the M1 segment of the β subunit. *Biochemistry* 36:15856–64
109. Wilson GG, Karlin A. 1998. The location

of the gate in the acetylcholine receptor. *Neuron* 20:1269–81
110. Hille B. 1992. *Ion Channels of Excitable Membranes.* Sunderland, MA: Sinauer
111. Charnet P, Labarca C, Leonard RJ, Vogelaar NJ, Czyzyk L, et al. 1990. An open-channel blocker interacts with adjacent turns of alpha-helices in the nicotinic acetylcholine receptor. *Neuron* 2:87–95
112. Imoto K, Methfessel C, Sakmann B, Mishina M, Mori Y, et al. 1986. Location of a delta-subunit region determining ion transport through the acetylcholine receptor channel. *Nature* 324:670–74
113. Villarroel A, Sakmann B. 1992. Threonine in the selectivity filter of the acetylcholine receptor channel. *Biophys. J.* 62:196–205
114. Wang F, Imoto K. 1992. Pore size and negative charge as structural determinants of permeability in the *Torpedo* nicotinic acetylcholine receptor channel. *Proc. R. Soc. London Ser. B* 250:11–17
115. Cohen BN, Labarca C, Czyzyk L, Davidson N, Lester HA. 1992. Tris + /Na + permeability ratios of nicotinic acetylcholine receptors are reduced by mutations near the intracellular end of the M2 region. *J. Gen. Physiol.* 99:545–72
115. (a) Dani JA. 1989. Open channel structure and ion binding sites of the nicotinic acetylcholine receptor channel. *J. Neurosci.* 9:884–92
116. Imoto K, Busch C, Sakmann B, Mishina M, Konno T, et al. 1988. Rings of negatively charged amino acids determine the acetylcholine receptor channel conductance. *Nature* 335:645–48
117. Bertrand D, Galzi JL, Devillers-Thiéry A, Bertrand S, Changeux JP. 1993. Mutations at two distinct sites within the channel domain M2 alter calcium permeability of neuronal alpha7 nicotinic receptor. *Proc. Natl. Acad. Sci. USA* 90:6971–75
118. Galzi JL, Devillers-Thiéry A, Hussy N, Bertrand S, Changeux JP, Bertrand D. 1992. Mutations in the ion channel domain of a neuronal nicotinic receptor convert ion selectivity from cationic to anionic. *Nature* 359:500–5
119. Corringer PJ, Bertrand S, Galzi JL, Devillers-Thiéry A, Changeux JP, Bertrand D. 1999. Mutational analysis of the charge selectivity filter of the alpha7 nicotinic acetylcholine receptor. *Neuron* 22:831–43
120. Wang CT, Zhang HG, Rocheleau TA, ffrench-Constant RH, Jackson MB. 1999. Cation permeability and cation-anion interactions in a mutant GABA-gated chloride channel from *Drosophila*. *Biophys. J.* 77:691–700
121. Armstrong CM, Hille B. 1998. Voltage-gated ion channels and electrical excitability. *Neuron* 20:371–80
122. Doyle DA, Cabral JM, Pfuetzner RA, Kuo A, Gulbis JM, et al. 1998. The structure of the potassium channel: molecular basis of K + conduction and selectivity. *Science* 280:69–77
123. Heinemann SH, Terlau H, Stuhmer W, Imoto K, Numa S. 1992. Calcium channel characteristics conferred on the sodium channel by single mutations. *Nature* 356:441–43
124. Opella SJ, Marassi FM, Gesell JJ, Valente AP, Kim Y, et al. 1999. Structures of the M2 channel-lining segments from nicotinic acetylcholine and NMDA receptors by NMR spectroscopy. *Nat. Struct. Biol.* 6:374–79
125. Adcock C, Smith GR, Sansom MS.P. 1998. Electrostatics and the ion selectivity of ligand gated channels. *Biophys. J.* 75:1211–22
126. Tikhonov DB, Zhorov BS. 1998. Kinked-helices model of the nicotinic acetylcholine receptor ion channel and its complexes with blockers: simulation by the Monte Carlo minimization method. *Biophys. J.* 74:242–55
127. Ortells MO, Barrantes GE, Wood C, Lunt GG, Barrantes FJ. 1997. Molecular modeling of the nicotinic acetylcholine recep-

tor transmembrane region in the open state. *Protein Eng.* 10:511–17
128. Chang G, Spencer RH, Lee AT, Barclay MT, Rees DC. 1998. Structure of the MscL homolog from *Mycobacterium tuberculosis:* a gated mechanosensitive ion channel. *Science* 282:2220–26
129. Lindqvist Y, Schneider G. 1997. Circular permutations of natural protein sequences: structural evidence. *Curr. Opin. Struct. Biol.* 7:422–27
130. Herz JM, Johnson DA, Taylor P. 1989. Distance between the agonist and noncompetitive inhibitor sites on the nicotinic acetylcholine receptor. *J. Biol. Chem.* 264:12439–48
131. Heidmann T, Changeux JP. 1980. Interaction of a fluorescent agonist with the membrane-bound acetylcholine receptor from *Torpedo marmorata* in the millisecond time range: resolution of an ''intermediate'' conformational transition and evidence for positive cooperative effects. *Biochem. Biophys. Res. Commun.* 97:889–96
132. Neubig RR, Cohen JB. 1980. Permeability control by cholinergic receptors in *Torpedo* post-synaptic membranes: agonist dose response relations measured at second and millisecond times. *Biochemistry* 19:2770–79
133. Colquhoun D, Sakmann B. 1985. Fast-events in single-channel currents activated by acetylcholine and its analogues at the frog muscle endplate. *J. Physiol.* 369:501–7
134. Edelstein SJ, Schaad O, Henry E, Bertrand D, Changeux JP. 1996. A kinetic mechanism for nicotinic acetylcholine receptor based on multiple allosteric transitions. *Biol. Cybern.* 75:361–79
135. Changeux JP, Edelstein SJ. 1998. Allosteric receptors after 30 years. *Neuron* 21:959–80
136. Colquhoun D, Sakmann B. 1998. From muscle endplate to brain synapses: a short history of synapses and agonist-activated ion channels. *Neuron* 20:381–87
137. Perutz MF. 1989. Mechanisms of cooperativity and allosteric regulation in proteins. *Quart. Rev. Biophys.* 22:139–236
138. Brunori M. 1999. Hemoglobin is an honorary enzyme. *Trends Biochem. Sci.* 24:158–61
139. Galzi JL, Revah F, Bouet F, Ménez A, Goeldner M, et al. 1991. Allosteric transitions of the acetylcholine receptor probed at the amino acid level with a photolabile cholinergic ligand. *Proc. Natl. Acad. Sci. USA* 88:5051–55
140. Chen J, Zhang Y, Akk G, Sine S, Auerbach A. 1995. Activation kinetics of recombinant mouse nicotinic acetylcholine receptors: mutations of alpha-subunit tyrosine 190 affect both binding and gating. *Biophys. J.* 69:849–59
141. Akk G, Zhou M, Auerbach A. 1999. A mutational analysis of the acetylcholine receptor channel transmitter binding site. *Biophys. J.* 76:207–18
142. Sine SM, Ohno K, Bouzat C, Auerbach A, Milone M, et al. 1995. Mutation of the acetylcholine receptor alpha subunit causes a slow-channel myasthenic syndrome by enhancing agonist binding affinity. *Neuron* 15:229–39
143. Akabas MH, Kaufmann C, Archdeacon P, Karlin A. 1994. Identification of acetylcholine receptor channel-lining residues in the entire M2 segment of the alpha subunit. *Neuron* 13:919–27
144. Revah F, Bertrand D, Galzi JL, Devillers-Thiéry A, Mulle C, et al. 1991. Mutations in the channel domain alter desensitization of a neuronal nicotinic receptor. *Nature* 353:846–49
145. Bertrand D, Devillers-Thiéry A, Revah F, Galzi JL, Hussy N, et al. 1992. Unconventional pharmacology of a neuronal nicotinic receptor mutated in the channel domain. *Proc. Natl. Acad. Sci. USA* 89:1261–65
146. Devillers-Thiéry A, Galzi JL, Bertrand S, Changeux JP, Bertrand D. 1992. Strati-

fied organization of the nicotinic acetylcholine receptor channel. *NeuroReport* 3:1001–4

147. Bertrand S, Devillers-Thiéry A, Palma E, Buisson B, Edelstein SJ, et al. 1997. Paradoxical allosteric effects of competitive inhibitors on neuronal alpha7 nicotinic receptor mutants. *NeuroReport* 8:3591–96
148. Labarca C, Nowak MW, Zhang H, Tang L, Deshpande P, Lester HA. 1995. Channel gating governed symmetrically by conserved leucine residues in the M2 domain of nicotinic receptors. *Nature* 376:514–16
149. Engel AG, Ohno K, Sine SM. 1999. Congenital myasthenic syndromes: recent advances. *Arch. Neurol.* 56:163–67
150. Léna C, Changeux JP. 1997. Pathological mutations of nicotinic receptors and nicotine-based therapies for brain disorders. *Curr. Opin. Neurobiol.* 7:674–82
151. Steinlein OK, Mulley JC, Propping P, Wallace RH, Phillips HA, et al. 1995. A missense mutation in the neuronal nicotinic acetylcholine receptor alpha 4 subunit is associated with autosomal dominant nocturnal frontal lobe epilepsy. *Nat. Genet.* 11:201–3
152. Steinlein OK, Magnusson A, Stoodt J, Bertrand S, Weiland S, et al. 1997. An insertion mutation of the CHRNA4 gene in a family with autosomal dominant nocturnal frontal lobe epilepsy. *Hum. Mol. Genet.* 6:943–47
153. Bertrand S, Weiland S, Berkovic SF, Steinlein OK, Bertrand D. 1998. Properties of neuronal nicotinic acetylcholine receptor mutants from humans suffering from autosomal dominant nocturnal frontal lobe epilepsy. *Br. J. Pharmacol.* 125:751–60
154. Kuryatov A, Gerzanich V, Nelson M, Olale F, Lindstrom J. 1997. Mutation causing autosomal dominant nocturnal frontal lobe epilepsy alters Ca2+ permeability, conductance, and gating of human alpha4beta2 nicotinic acetylcholine receptors. *J. Neurosci.* 17:9035–47
155. Lee YH, Li L, Lasalde J, Rojas L, McNamee M, et al. 1994. Mutations in the M4 domain of *Torpedo californica* acetylcholine receptor dramatically alter ion channel function. *Biophys. J.* 66:646–53
156. Bouzat C, Bren N, Sine SM. 1994. Structural basis of the different gating kinetics of fetal and adult acetylcholine receptors. *Neuron* 13:1395–402
157. Wang HL, Milone M, Ohno K, Shen XM, Tsujino A, et al. 1999. Acetylcholine receptor M3 domain: stereochemical and volume contributions to channel gating. *Nat. Neurosci.* 2:226–33
158. Lo DC, Pinkham JL, Stevens CF. 1991. Role of a key cysteine residue in the gating of the acetylcholine receptor. *Neuron* 6:31–40
159. England PM, Zhang Y, Dougherty DA, Lester HA. 1999. Backbone mutations in transmembrane domains of a ligand-gated ion channel: implications for the mechanism of gating. *Cell* 96:89–98
160. Campos-Caro A, Sala S, Ballesta JJ, Vicente-Agullo F, Criado M, Sala F. 1996. A single residue in the M2-M3 loop is a major determinant of coupling between binding and gating in neuronal nicotinic receptors. *Proc. Natl. Acad. Sci. USA* 93:6118–23
161. Croxen R, Newland C, Beeson D, Oosterhuis H, Chauplannaz G, et al. 1997. Mutations in different functional domains of the human muscle acetylcholine receptor alpha subunit in patients with the slow-channel congenital myasthenic syndrome. *Hum. Mol. Genet.* 6:767–74
162. Monod J, Wyman J, Changeux JP. 1965. On the nature of allosteric transitions: a plausible model. *J. Mol. Biol.* 12:88–118
163. Karlin A. 1967. On the application of ''a plausible model'' of allosteric proteins to the receptor for acetylcholine. *J. Theoret. Biol.* 16:306–20

164. Del Castillo J, Katz B. 1957. Interaction at endplate receptors between different choline derivatives. *Proc. R. Soc. London Ser. B* 146:369–81
165. Koshland D, Nemethy G, Filmer D. 1966. Comparison of experimental binding data and theoretical models in proteins containing subunits. *Biochemistry* 5:365–85
166. Galzi JL, Edelstein SJ, Changeux JP. 1996. The multiple phenotypes of allosteric receptor mutants. *Proc. Natl. Acad. Sci. USA* 93:1853–58
167. Alkondon M, Pereira EF, Eisenberg HM, Albuquerque EX. 1999. Choline and selective antagonists identify two subtypes of nicotinic acetylcholine receptors that modulate GABA release from CA1 interneurons in rat hippocampal slices. *J. Neurosci.* 19:2693–705

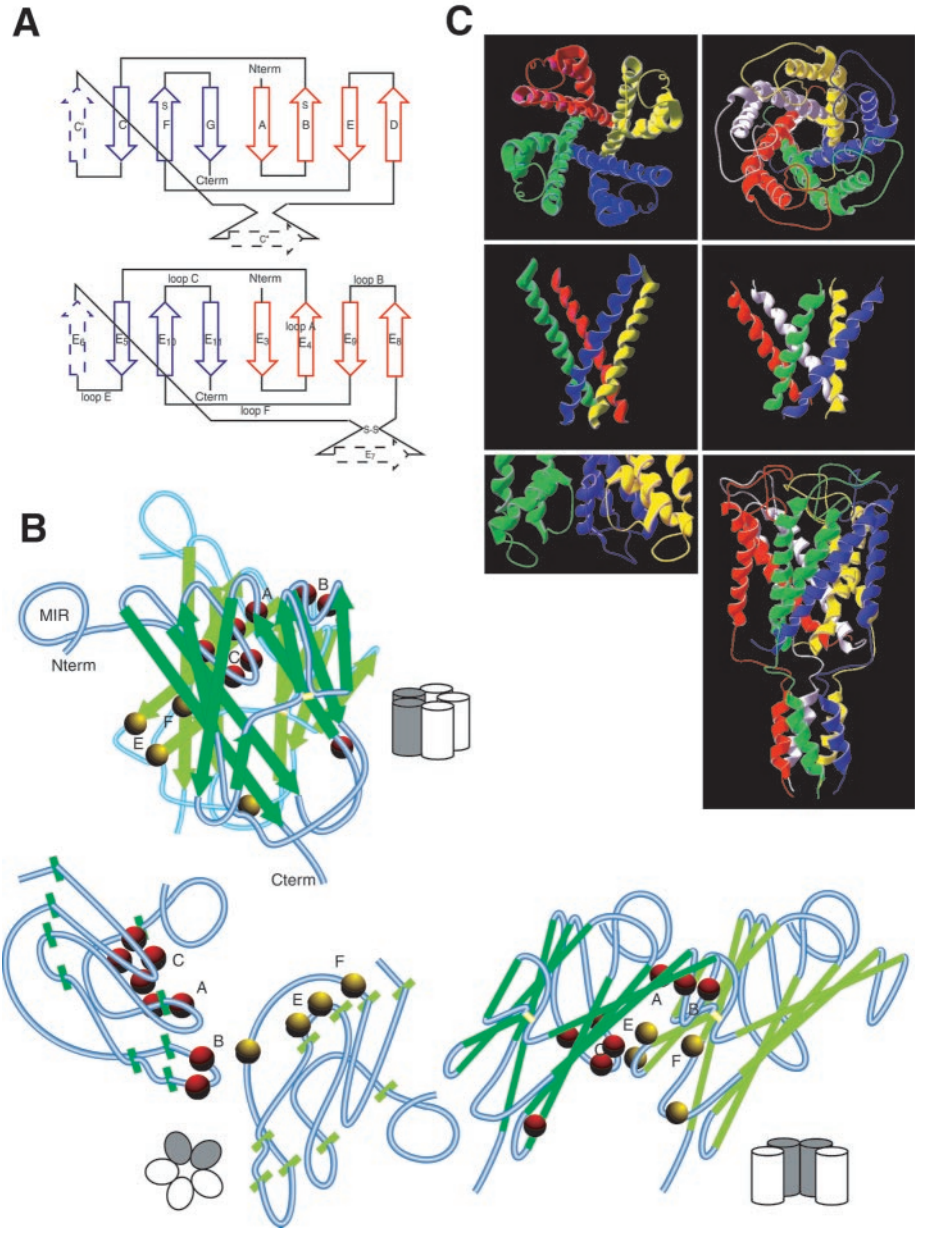

Figure 2 (*A, upper*) Topology cartoon of the immunoglobin (Ig) fold. (*Red strands*) The main sheet of the sandwich; (*blue strands*) the smallest sheet; (*dashed strands*) present only in the variable chains of the IgG. (*A, lower*) Topology cartoon of the proposed nicotinic fold. The strands are named according to Le Novère et al (46). (*B, upper*) Dimer of two subunits (*dark green and light green*) viewed from a line parallel to the membrane and perpendicular to the subunit interface. (*Red balls*) The residues of the main component of the ACh binding

site; (*yellow balls*) the residues of the complementary component. Note the tilt between the subunits in the plane of the interface. (*B, bottom left*) Dimer of subunits viewed from the extracellular side along a line perpendicular to the membrane. Note that the planes of the β-sheets do not contain the axis of symmetry of the receptor. (*B, lower right*) Dimer of subunits viewed from the pore of the receptor. Note the tilt from the vertical, which allows a possible interaction between the two extremities of extracellular domain from adjacent subunits. For sake of clarity, the lateral tilt presented in the *left panel* has been omitted. (*Small drawings*) The position of the represented subunits within the oligomer. (*C, left panels*) *Streptomyces lividans* potassium channel (1BL8). (*Top to bottom*) View from the extracellular side, lateral view of the inner helices, **and** view of the selectivity filter upside-down, as it could be in the nAChR. (*C, right panels*) *Mycobacterium tuberculosis* mechanosensitive channel (1MSL). (*Top to bottom*) View from the extracellular side, lateral view of the inner helices, lateral view of the complete channel. The pictures are screenshots of SWISSPDBVIEWER.